Chemical Engineering Journal 325 (2017) 249–256

Contents lists available at ScienceDirect

Chemical Engineering Journal

journal homepage: www.elsevier.com/locate/cej

# Encapsulation of aluminum nanoparticles within copper oxide matrix for enhancing their reactive properties

Ji Young Ahn [a], Soo Hyung Kim [a,b,c,*]

[a] Research Center for Energy Convergence Technology, Pusan National University, 2 Busandaehak-ro 63beon-gil, Geumjung-gu, Busan 46241, Republic of Korea
[b] Department of Nano Fusion Technology, Pusan National University, 2 Busandaehak-ro 63beon-gil, Geumjung-gu, Busan 46241, Republic of Korea
[c] Department of Nanoenergy Engineering, Pusan National University, 2 Busandaehak-ro 63beon-gil, Geumjung-gu, Busan 46241, Republic of Korea

## HIGHLIGHTS

- Al nanoparticles (NPs) are significantly oxidized by calcination process.
- CuO-encapsulated Al NPs are fabricated using a spray pyrolysis.
- CuO matrices protect Al NPs from thermal oxidation in the calcination process.
- The reactive properties of CuO-encapsulated Al NPs are much better than those of Al/CuO composites.

## ARTICLE INFO

*Article history:*
Received 6 March 2017
Received in revised form 9 May 2017
Accepted 10 May 2017
Available online 11 May 2017

*Keywords:*
Spray pyrolysis
Calcination
Nanoenergetic materials
Encapsulation
Ignition
Burn rate

## ABSTRACT

Simple and easy spray pyrolysis and subsequent calcination processes were employed in this study to fabricate nanoenergetic materials (nEMs) composed of Al as the fuel and CuO as the oxidizer. Al nanoparticles (NPs) and $Cu(NO_3)_2$ as the CuO precursor were first dissolved in ethanol, and then they were pyrolized in the gas phase. After the subsequent calcination process, $Cu(NO_3)_2$ and its intermediate matrix covering Al NPs were completely transformed to the CuO matrix by thermal decomposition, and thus, the CuO-encapsulated Al NPs were successfully fabricated. The burn rate of the CuO-encapsulated Al NPs fabricated in this study was found to be much higher than that of Al/CuO composite NPs, which were fabricated for comparison by traditional sonication mixing and subsequent calcination processes. The ignition delay time and total burning time of CuO-encapsulated Al NPs were also much shorter than those of Al/CuO composite NPs. This suggests that the combination of spray pyrolysis and subsequent calcination processes can be a versatile and effective method to form the homogeneous and intimate nEMs composed of fuel materials (i.e., Al NP core) and oxidizers (i.e., CuO matrix) with high reactivity and excellent combustion properties.



## 1. Introduction

Energetic materials (EMs) possess chemical enthalpy, which can be rapidly turned into thermal energy when they are initiated by an external energy input. Generally, there are two types of EMs [1]: The first type, namely, the monomolecular EMs have the fuel and oxidizer within a molecule, e.g., nitrocellulose and nitroglycerine, which are generally produced by the combination of nitration [2–4], dehydration [5–8], and polymerization [9,10] processes. These EMs generate high power and exhibit a high energy release rate, which are strongly dependent on the chemical kinetics, the fuel and oxidizer balance, and the physical density of materials. The second type, i.e., the composite EMs are a mixture of fuel and oxidizer particles at the micro- and nanoscales. The composite EMs are produced by various physical mixing processes, such as milling [11–14], sonic wave-assisted physical mixing [15–21], sol-gel chemistry [22–24], electrostatic assembly [25], and molecular self-assembly [26]. The composite EMs generally exist in the form of powders. The energy release rate and combustion properties of composite EMs can be controlled by manipulating the rate of mass transfer between the reactants.

Various fabricating methods for composite nanoscale energetic materials (nEMs) have been developed because of their highly exothermic reactions compared to microscale energetic materials. In various nEM formulations, aluminum (Al) as a relatively stable

* Corresponding author at: Research Center for Energy Convergence Technology, Pusan National University, 2 Busandaehak-ro 63beon-gil, Geumjung-gu, Busan 46241, Republic of Korea.
*E-mail address:* sookim@pusan.ac.kr (S.H. Kim).

http://dx.doi.org/10.1016/j.cej.2017.05.066
1385-8947/

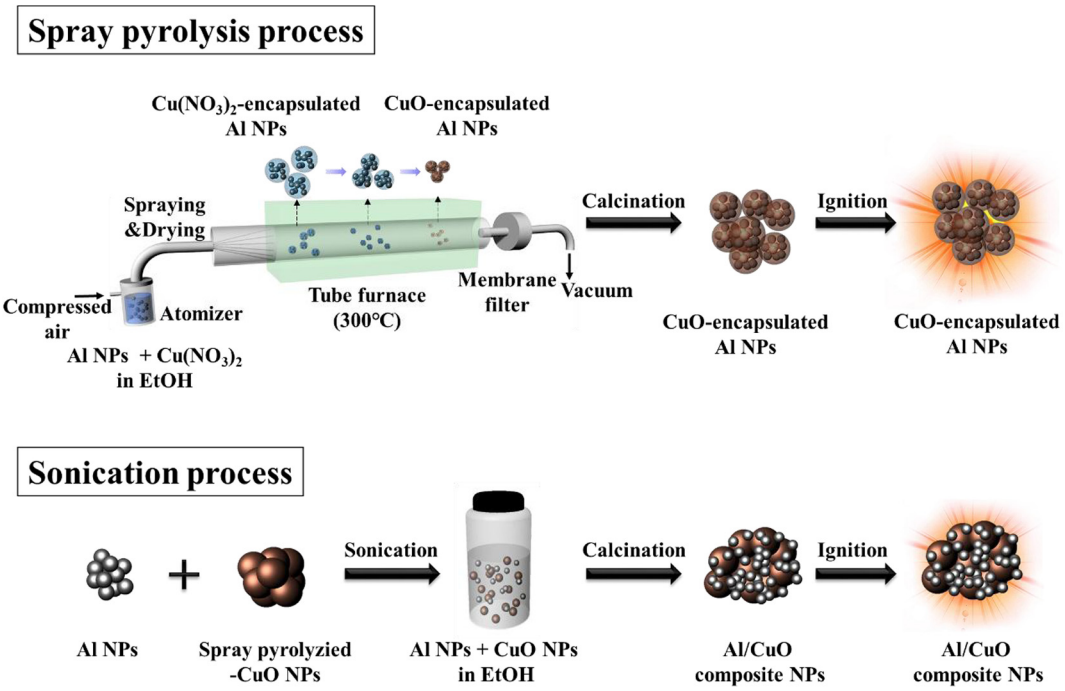


**Fig. 1.** Schematics of spray pyrolysis and sonication processes for fabricating CuO-encapsulated and Al/CuO composite nanoparticles (NPs), respectively, and their ignition and combustion properties after subsequent calcination process.

fuel metal is widely used in combination with various metal oxides [27–32]. Once the nEMs are ignited, a self-sustained exothermic reaction occurs within a fraction of a second. Therefore, the nEMs can be applied to thermal engineering, as explosives, propulsion fuels, and pyrotechnics for both civilian and military purposes [33–36]. In order to increase the energy release rate and combustion properties of nEMs, the degree of intermixing needs to be increased and the size of reactants should be decreased under the conditions of fixed chemical composition and mixing ratio of reactants. However, the aforementioned physical mixing methods experience inherent difficulties in fabricating uniformly intermixed nEMs neighboring at nanoscale distance [37]. Therefore, the encapsulation of fuel metal particles by metal oxidizers is a potential method to enhance the combustion properties of nEMs due to intimate contact between the fuel and oxidizer.

In this work, we demonstrate a versatile, simple and easy to scale-up method to fabricate nanoscale EMs (nEMs) using spray pyrolysis and subsequent calcination processes. With the use of the spray pyrolysis method, we can specifically employ metal (e.g., Al NPs) fuel seeds and metal nitrate (e.g., $Cu(NO_3)_2$) oxidizer precursor matrices, which are finally turned into a metal oxide (e.g., CuO) by subsequent calcination process. Thus, the CuO-encapsulated Al NPs are the final product fabricated in this study. We also have systematically investigated the effect of calcination conditions on the ignition and combustion properties of CuO-encapsulated Al NPs fabricated by the spray pyrolysis method. Further, the ignition and combustion properties of Al/CuO composite-based nEMs fabricated by the traditional sonication-based mixing and subsequent calcination processes are also examined for comparison.

## 2. Experimental details

Al NPs were commercially available from Nano Technology, Ltd. (Korea). They had an average size of approximately 80 nm and were used as the fuel metal without further treatment. In order

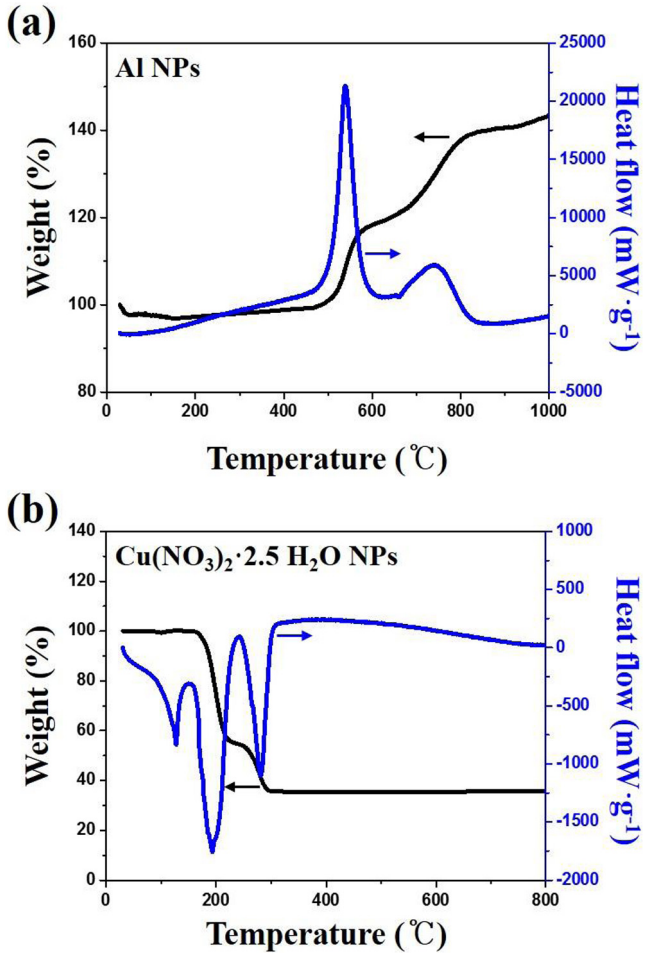


**Fig. 2.** Results of DSC and TGA analyses for (a) Al NPs and (b) $Cu(NO_3)_2{\cdot}2.5H_2O$ NPs.

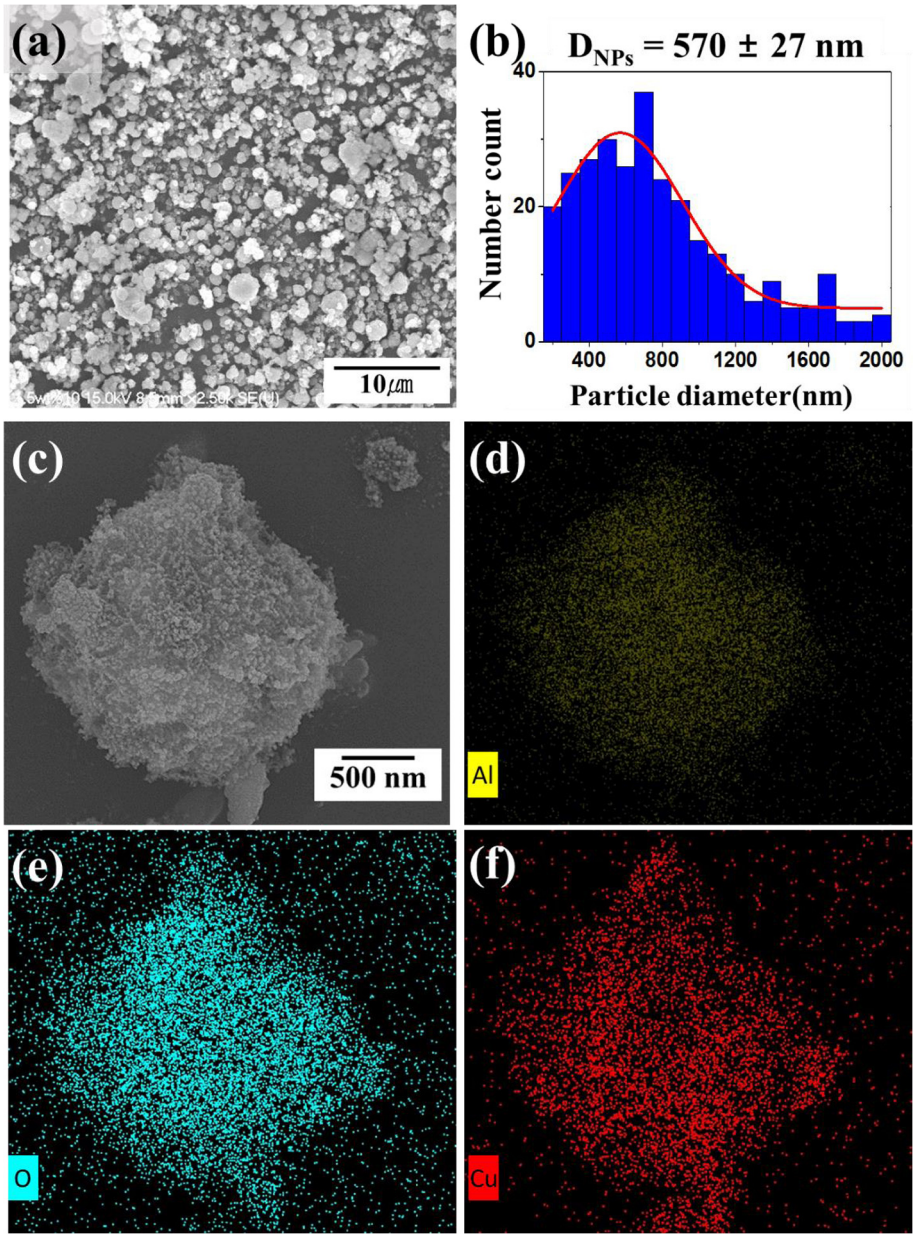


**Fig. 3.** (a) LR-SEM image, (b) particle size distribution and average particle size, and (c) HR-SEM image of CuO-encapsulated Al NPs. The elemental mapping images of (d) Al, (e) O, and (f) Cu of CuO-encapsulated Al NPs.

to fabricate Al and CuO composite particles, spray pyrolysis and subsequent calcination processes were employed, as depicted in Fig. 1. Briefly, copper nitrate ($Cu(NO_3)_2{\cdot}2.5H_2O$, Sigma Aldrich) and Al NPs were dispersed in an ethanol solution with the mixing ratio of Al:$Cu(NO_3)_2{\cdot}2.5H_2O$ = 30:70 wt%. The precursor solution was then aerosolized using an atomizer that was operated using compressed air at 35 psi, and the solvent in the micro-sized aerosol droplets was then removed by passing them through a silica-gel drier. The copper nitrate-encapsulated Al NPs were then continuously oxidized by passing them through a quartz tube reactor enclosed in a tube furnace heated at 300 °C. The residence time of aerosol particles during spray pyrolysis was ~1 s. The resulting CuO-encapsulated Al NPs formed were collected on a membrane filter with a pore size of 200 nm, and then, they were subsequently calcined at 300 °C in a closed box furnace with various calcination durations. For comparison, we also fabricated Al/CuO composite EMs using a sonication mixing process followed by the calcination process. Briefly, $Cu(NO_3)_2{\cdot}2.5H_2O$ was dissolved in an ethanol solution without Al NPs and then aerosolized by a standard atomizer. The aerosolized copper nitrate-containing droplets were passed through a silica-gel dryer and then continuously introduced into the tube furnace heated at 300 °C for converting them into CuO NPs via thermal decomposition. The as-prepared CuO NPs were then mixed with Al NPs in an ethanol solution and then calcined for various calcination durations at 300 °C.

Both the CuO-encapsulated Al NPs and Al/CuO composite NPs fabricated in this study were characterized by various techniques, including thermogravimetric analysis and differential scanning calorimetry (TGA and DSC; Setaram, Model No. LABSYS evo) at temperatures ranging from 20 to 1000 °C at 10 °C/min, X-ray diffractometry (XRD; Philips, X'pert PRO MRD) using Cu Kα radiation, scanning electron microscopy (SEM; Hitachi S4700) operated at 15 kV, and Cs-corrected scanning transmission electron microscopy (STEM; JEOL, JEM-2100) operated at 200 kV. In order to

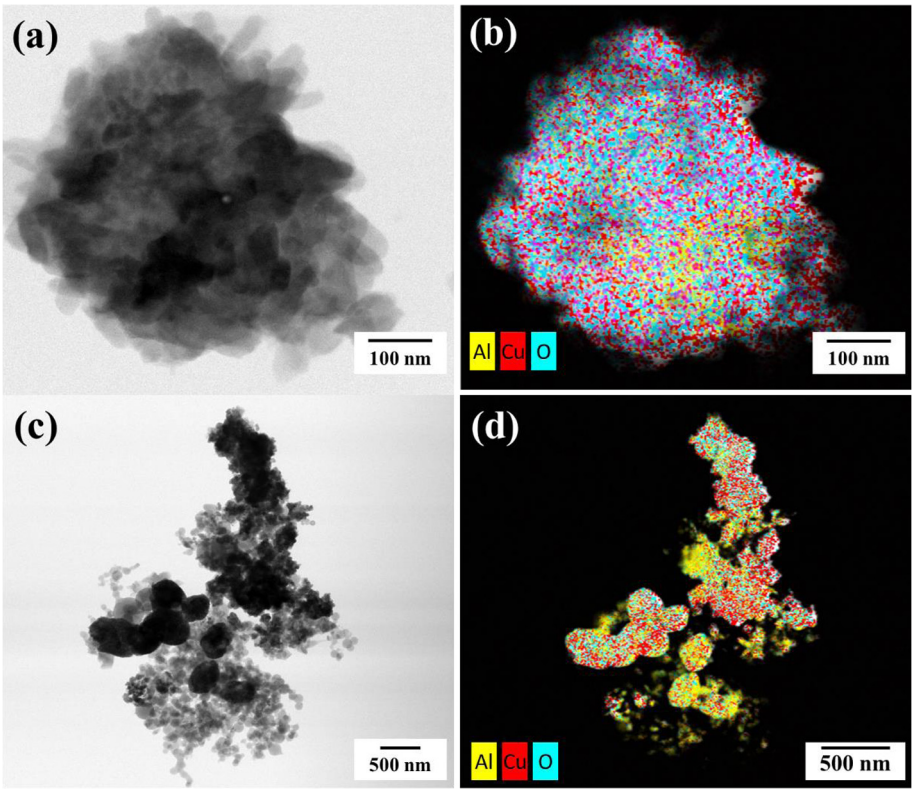


**Fig. 4.** (a) STEM and (b) elemental mapping image of CuO-encapsulated Al NPs. (c) STEM and (d) element mapping image of Al/CuO composite NPs.

observe the ignition, combustion, and explosion characteristics of the composite EMs fabricated in this study, a high-speed camera (Fastcam SA3 120 K, Photron) was used with a minimum and maximum frame rate of 60 and 1,200,000 fps, respectively, 17.4 mm × 17.4 mm CMOS image sensor, pixel size of 17 μm × 17 μm, and operating voltage and current of AC 100–240 V and 60 A, respectively. The explosive force was measured using a pressure-cell tester system, in which the pressure generated by the thermal ignition of the composite powder was automatically measured by a pressure sensor (PCB Piezotronics, Model No. 113AO3). The distance between the composite powder and pressure sensor was ~2 cm. The pressure was amplified by in-line charge amplifiers (Model No. 422E11, PCB Piezotronics) and transformed into an electric signal by a signal conditioner (Model No. 480C02, PCB Piezotronics) with the frequency response of 25 kHz. This signal was recorded by an oscilloscope (Tektronix, Model No. TDS 2012B). Approximately 13 mg composite powder was placed in the pressure-cell tester, and the tungsten hot-wire connected to a power transformer was inserted. The pressure cell was completely sealed, and then voltage was applied. The tungsten hot-wire was rapidly heated and the loaded composite powder was ignited. After pressure was generated by the explosion and gas evolution of the composite powder within the pressure cell, the converted electrical signal was recorded in situ in terms of the time-to-pressure graph in the oscilloscope.

## 3. Results and discussion

The thermal properties of composite materials fabricated in this study were measured using TGA and DSC. Fig. 2a and b show the TGA and DSC results at temperatures ranging from 20 to 1000 °C varied at 10 °C/min under air flow for Al NPs and $Cu(NO_3)_2{\cdot}2.5H_2O$ NPs, respectively. As shown in Fig. 2a, the mass of Al NPs did not appreciably change until 500 °C, and it was then suddenly increased at >500 °C. The heat flow of Al NPs increased gradually up to 500 °C, and then, it showed a strongly exothermic reaction at ~550 °C due to the oxidation of Al NPs. Thereafter, the second exothermic reaction at ~750 °C occurred. It is presumably because Al partially remained were completely oxidized near or higher than the melting point of Al NPs (≥660 °C) [38]. Generally, $Cu(NO_3)_2{\cdot}2.5H_2O$ is known to convert to CuO through three steps. As shown in Fig. 2b, several endothermic reactions were observed for $Cu(NO_3)_2{\cdot}2.5H_2O$ NPs. The first endothermic reaction peak indicated the phase change from $Cu(NO_3)_2{\cdot}2.5H_2O$ to $Cu_2(NO_3)_2(OH)_2$ at 110–150 °C. The second endothermic reaction peak indicated the phase change from $Cu_2(NO_3)_2(OH)_2$ to $CuO{\cdot}CuONO_3$ at 170–220 °C. The third endothermic reaction peak indicated the phase change from $CuO.CuONO_3$ to CuO at 280–320 °C [39–42]. The mass ratio of CuO to $Cu(NO_3)_2{\cdot}2.5H_2O$ (i.e., $M_{CuO}/M_{Cu(NO3)2{\cdot}2.5H2O}$; here, $M_{CuO}$ = 79.545 g $mol^{-1}$, $M_{Cu(NO3)2{\cdot}2.5H2O}$ = 232.591 g·$mol^{-1}$) was estimated to be approximately 0.34. From the simple calculation of mass ratio, we expected that the $Cu(NO_3)_2{\cdot}2.5H_2O$ was completely converted to CuO at ~300 °C. This suggests that Al NPs are not strongly affected by the heating process during the spray pyrolysis and subsequent calcination processes at ~300 °C, during which $Cu(NO_3)_2$ NPs are converted to CuO.

Low-resolution SEM image in Fig. 3a show the morphology of the CuO-encapsulated Al NPs fabricated by spray pyrolysis and subsequent calcination processes at 300 °C for 40 min. The as-prepared CuO-encapsulated Al NPs are spherical with an average diameter of 570 ± 27 nm as shown in Fig. 3b. Fig. 3c–f show the high resolution SEM and elemental mapping images: It was clearly observed that Cu (red) and O (blue) were predominant elements, and the relatively small amount of Al (yellow) was present. This confirms that Al NPs were encapsulated by CuO matrix by spray pyrolysis and subsequent calcination processes in this study. This was also corroborated by STEM analysis. Fig. 4a and b shows that

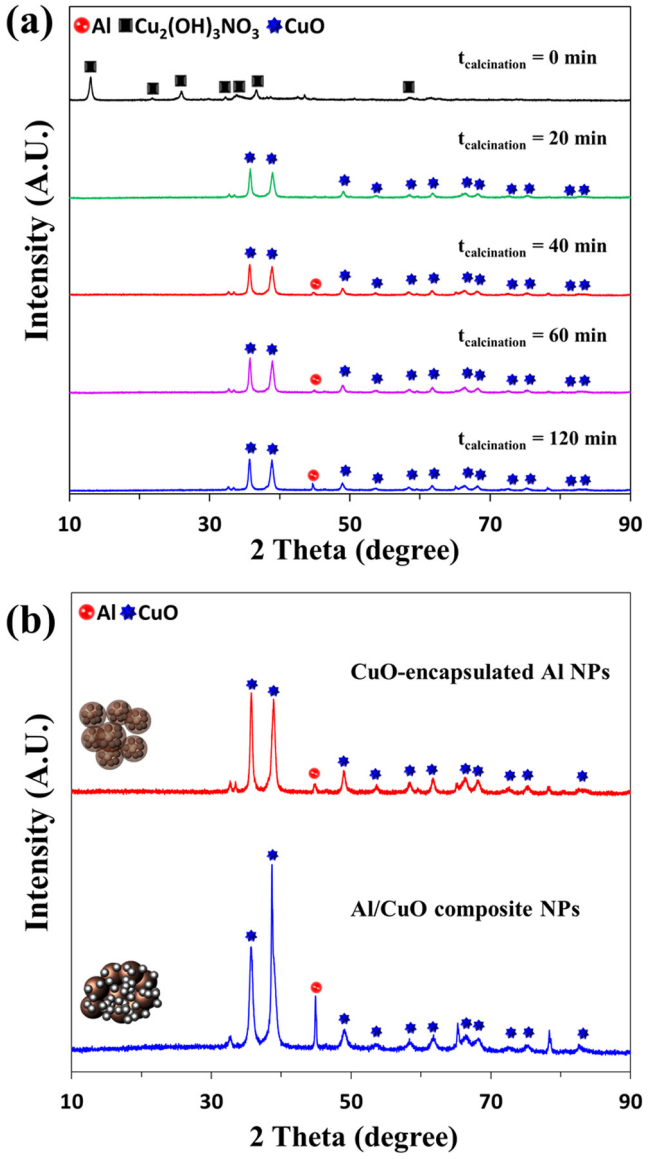


**Fig. 5.** XRD analyses for (a) CuO-encapsulated Al NPs calcined at various durations, and (b) the comparison of XRD results for CuO-encapsulated Al NPs and Al/CuO composite NPs calcined at 40 min.

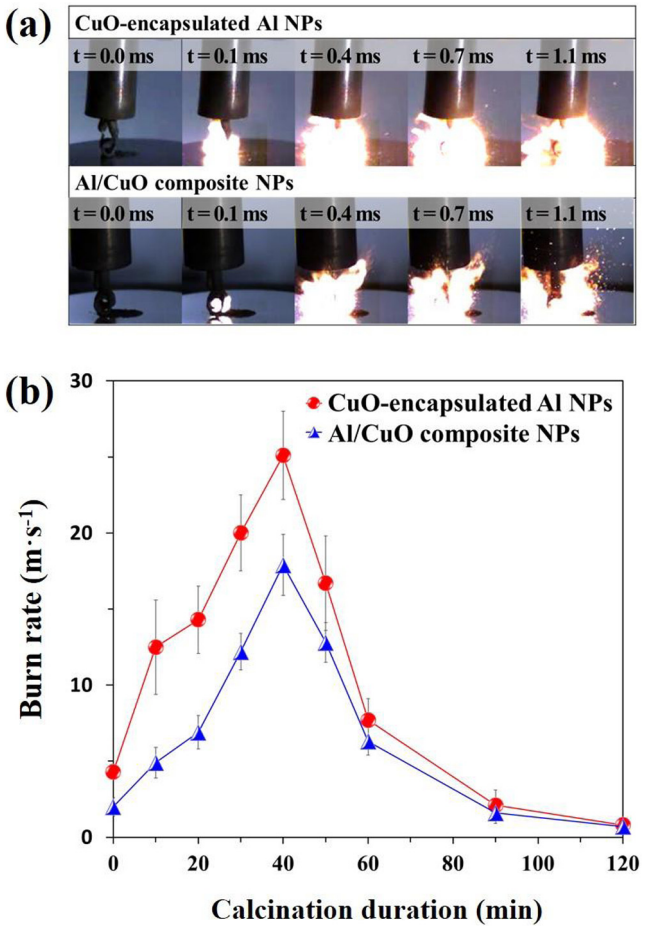


**Fig. 6.** (a) Photographs of ignition and combustion reactions of CuO-encapsulated Al NPs and Al/CuO composite NPs calcined for 40 min. (b) The evolution of burn rates of CuO-encapsulated Al NPs and Al/CuO composite NPs as a function of calcination duration.

Al NPs (yellow) were encapsulated by the CuO matrix (blue and red). This also suggests that Al and CuO components were in close contact at the nanoscale. For comparison, Fig. 4c and d show the scanning TEM and elemental mapping images for the Al/CuO composite NPs prepared by simple sonication and subsequent calcination processes, in which Al NPs and CuO NPs were observed to be homogeneously mixed.

As the calcination duration increased, the formation of crystallite CuO structures was clearly observed by performing XRD measurement as shown in Fig. 5a. However, the presence of Al was rarely observed due to the encapsulation of CuO matrix. To identify the effect of CuO encapsulation on Al NPs, we also performed XRD analyses for both CuO-encapsulated Al NPs and Al/CuO composite NPs as shown in Fig. 5b. As the results, it was observed that the signal originated from Al was very weak for the case of CuO-encapsulated Al NPs because the Al NPs were protected by CuO matrix. However, the strong signals originated from both Al and CuO were clearly appeared for the case of Al/CuO composite NPs, in which Al and CuO were physically mixed so that Al and CuO NPs were separately exposed. This was also corroborated by the SEM, TEM, and elemental mapping results that Al NPs are sufficiently encapsulated by the formation of CuO matrix in the spray pyrolysis and subsequent calcination processes.

The hot-wire ignition and combustion properties for both the CuO-encapsulated Al NPs and Al/CuO composite NPs calcined for 40 min measured using the photographs obtained from a high-speed camera are shown in Fig. 6a. The ignition delay time and total burning time for the CuO-encapsulated Al NPs were ~0.9 ± 0.2 s and ~5.17 ± 0.32 ms, while those for Al/CuO composite NPs were ~1.8 ± 0.5 s and ~9.53 ± 0.2 ms, respectively. This suggests that the reactivity properties of CuO-encapsulated Al NPs are considerably superior to those of Al/CuO composite NPs. This was corroborated by systematically examining the burn rates of particles as a function of the calcination duration, as shown in Fig. 6b. The burn rates of CuO-encapsulated Al NPs prepared by spray pyrolysis and subsequent calcination processes increased with the calcination duration up to 40 min due to the complete thermal decomposition of residual copper nitrate intermediates. Then, it significantly decreased at the calcination duration >40 min due to the serious oxidation of Al NPs, which was also corroborated later by STEM analyses results, as shown in Fig. 7. However, the burn rates of Al/CuO composite NPs were much lower than those of CuO-encapsulated Al NPs at the same calcination duration. This suggests that CuO matrices formed by spray pyrolysis protect the Al core NPs from serious oxidation to some extent.

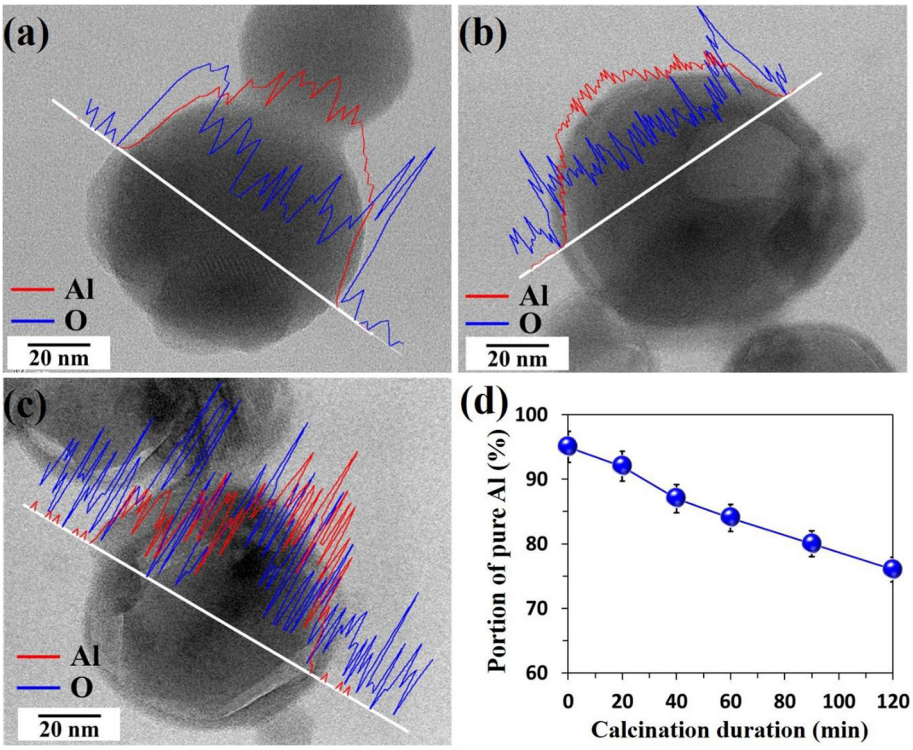


**Fig. 7.** TEM images of Al NPs with various calcination durations: (a) 0 min, (b) 40 min, and (c) 120 min. (d) Calculated portion of pure Al NPs as a function of the calcination duration.

The possible reason for the decrease in the burn rates for longer calcination durations, i.e., >40 min for both the CuO-encapsulated Al NPs and Al/CuO composite NPs is the significant oxidation of Al NPs.

We performed STEM analyses to examine the effect of various calcination durations at a fixed calcination temperature of 300 °C on the thickness of the oxide layer formed on the surface of Al NPs; the results are shown in Fig. 7. The portion of pure Al was simply calculated by following Eq. (1).

$$\text{Portion of pure Al} = \frac{\frac{4}{3}\pi r_{Al^3}}{\frac{4}{3}\pi r_{Al} + Al_2O_3^3} \times 100 \quad (1)$$

Here, $r_{Al}$ is the radius of Al NP and $r_{Al+Al2O3}$ is the radius of Al NP with the $Al_2O_3$ layer. It was clearly seen that an increase in the calcination duration resulted in an increase in the oxide layer thickness. Since the average size of Al NPs is approximately 80 nm and the thickness of the oxide layer is approximately 3 nm in the case of Al NPs that were not subjected to calcination (i.e., $t_{calcination}$ = 0 min, Fig. 7a), the portion of pure Al is determined to be ~95%. For $t_{calcination}$ = 40 and 120 min (see Fig. 7b and c), the thicknesses of the oxide layers on the surface of Al NPs were ~6 and ~10 nm, respectively, which resulted in a significant reduction in the portion of pure Al to ~87% and ~76%, respectively. Fig. 7d summarizes the evolution of the portion of pure Al NPs with varying calcination duration.

Fig. 8a shows the pressure traces of both the CuO-encapsulated Al NPs and Al/CuO composite NPs when they were ignited in the pressure-cell tester system. The magnitude of the pressure rise of CuO-encapsulated Al NPs is approximately 6 times greater than that of Al/CuO composite NPs. Fig. 8b shows the pressurization rate, which was determined by calculating the ratio of the maximum pressure to the rise time. The pressurization rate of CuO-encapsulated Al NPs was ~0.68 kPa $\mu s^{-1}$, which is approximately 17 times higher than that of Al/CuO composite NPs

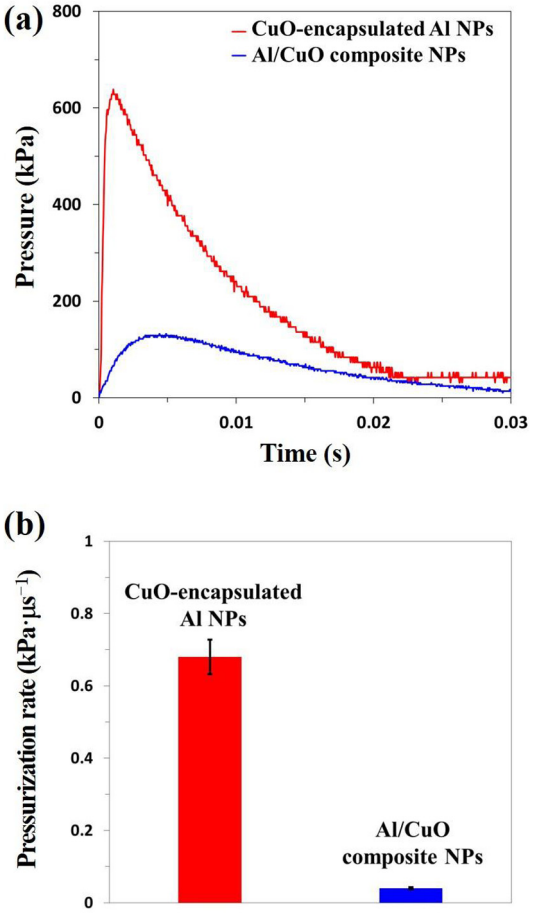


**Fig. 8.** (a) Pressure trace and (b) pressurization rate of CuO-encapsulated Al NPs and Al/CuO composite NPs calcined for 40 min.

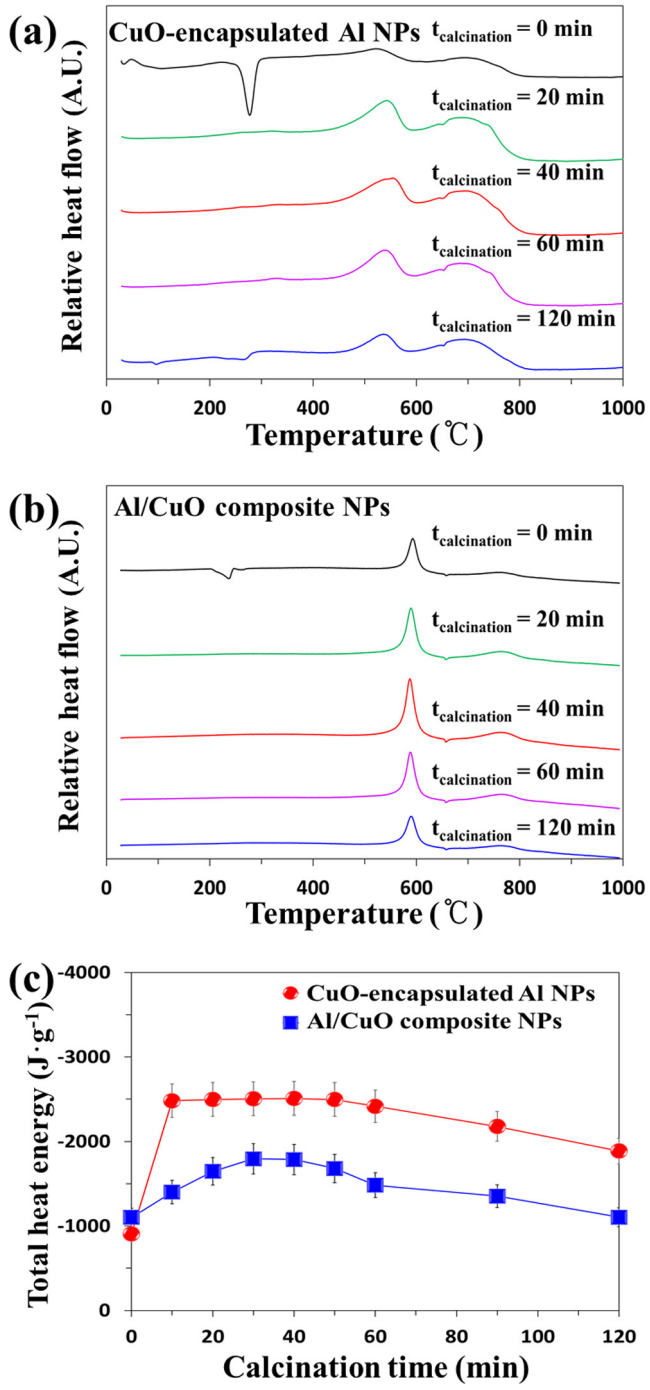


**Fig. 9.** Results of DSC analyses for (a) CuO-encapsulated Al NPs and (b) Al/CuO composite NPs. (c) The total heat energy generated by CuO-encapsulated NPs and Al/CuO composite NPs.

(i.e., 0.04 kPa $\mu s^{-1}$). This suggests that the spray pyrolysis and subsequent calcination processes employed in this study are very effective in fabricating nEMs with higher reactivity and combustion properties.

Fig. 9 shows the results of DSC analyses for both CuO-encapsulated Al NPs and Al/CuO composite NPs by varying the calcination duration at the fixed temperature of ~300 °C. Fig. 9a presents the results of DSC analysis to examine the effect of the calcination duration on the heat energy released by CuO-encapsulated Al NPs. In the case of the CuO-encapsulated Al NPs fabricated by spray pyrolysis without calcination (i.e., $t_{calcination}$ = 0 min), the endothermic reaction occurred due to the thermal decomposition of residual intermediate $Cu_2(OH)_3NO_3$. After calcination over a sufficient period (i.e., $t_{calcination} \geq 20$ min), the endothermic reaction disappeared and exothermic reactions were occurred between 500 and 800 °C for calcination durations of 20–120 min. However, the exothermic reaction of the Al/CuO composite NPs occurred between 570 and 800 °C, as shown in Fig. 9b. The possible reason for the exothermic reactions occurring at the higher temperature of ~570 °C for the Al/CuO composite NPs is because Al NPs were also oxidized to some extent during the calcination process; this resulted in a decrease in the intensity of the exothermic reaction with increasing calcination duration, as shown in Fig. 9c, which shows the evolution of the total heat energy (ΔH) released by CuO-encapsulated Al NPs and Al/CuO composite NPs at different calcination durations. The total heat energy released from CuO-encapsulated Al NPs without calcination was ~907 J·g$^{-1}$. It then significantly increased up to the calcination duration of 50 min (ΔH = ~2500 J·g$^{-1}$), after which it gradually decreased. This suggests that the encapsulation within the CuO matrices protects Al NPs from serious oxidation to some extent, so the combustion properties of CuO-encapsulated Al NPs were superior. However, the long calcination durations over 40 min can deteriorate the combustion properties of CuO-encapsulated Al NPs due to the resultant substantial oxidation of Al NPs. The total heat energy released by Al/CuO composite NPs showed a trend similar to that shown by CuO-encapsulated Al NPs. However, the magnitude of total heat energy for the CuO-encapsulated Al NPs was significantly higher than that for the Al/CuO composite NPs. This suggests that the spray pyrolysis process employed in this study is very effective in the fabrication of nEMs with homogeneous mixtures of a fuel (Al NPs) and an oxidizer (CuO matrix), and the optimized subsequent calcination process enhances their combustion properties via the complete thermal decomposition of the oxidizer matrices, which can simultaneously protect the oxidation of core fuel materials.

## 4. Conclusions

In this work, we have demonstrated simple and easy spray pyrolysis and subsequent calcination processes to fabricate Al and CuO-based nEMs with enhanced reactivity and combustion properties. The CuO-encapsulated Al NPs fabricated by spray pyrolysis were found to be homogeneously mixed with a nEM structure composed of Al NP cores surrounded by CuO matrices. They were then optimized by the subsequent calcination process (i.e., $t_{calcination}$ = 40 min at 300 °C), which enabled the completion of the thermal decomposition of the oxidizer matrices. The reactivity and combustion properties of CuO-encapsulated Al NPs fabricated by the combination of spray pyrolysis and optimized calcination processes were found to be superior because of the successful formation of homogeneous mixtures composed of Al NPs (fuel) and CuO matrices (oxidizer) in close contact. However, the longer calcination durations (i.e., $t_{calcination}$ > 40 min at 300 °C) resulted in a significant reduction in the burn rates for both CuO-encapsulated Al NPs and Al/CuO composite NPs because of the substantial oxidation of Al NPs. Therefore, the combination of spray pyrolysis and optimized calcination processes employed in this study can be an effective method to fabricate highly reactive nEMs with enhanced combustion properties.

## Acknowledgments

This study was financially supported by the 2014 Post-Doc. Development Program of Pusan National University. This study was also partially supported by the Civil & Military Technology

Cooperation Program through the National Research Foundation of Korea (NRF) funded by the Ministry of Science, ICT & Future Planning (No. 2013M3C1A9055407).

## References


[1] U. Teipel, Energetic Materials: Particle Processing and Characterization, WILEY-VCH Verlag GmbH & Co. KGaA, Germany, 2005.
[2] P.F. Pagoria, G.S. Lee, A.R. Mitchell, R.D. Schmidt, A review of energetic materials synthesis, Thermochim. Acta. 384 (2002) 187–204.
[3] A.K. Sikder, N. Sikder, A review of advanced high performance, insensitive and thermally stable energetic materials emerging for military and space applications, J. Hazard. Mater. 112 (2004) 1–15.
[4] D.M. Badgujar, M.B. Talawar, S.N. Asthana, P.P. Mahulikar, Advances in science and technology of modern energetic materials: an overview, J. Hazard. Mater. 151 (2008) 289–305.
[5] V. Thottempudi, F. Forohor, D.A. Parrish, J.M. Shreeve, Tris (triazolo) benzene and its derivatives: high density energetic materials, Angew. Chem. Int. Ed. Engl. 51 (2012) 9881–9885.
[6] E.C. Mattos, E.D. Moreira, R.C. Dutra, M.F. Diniz, A.P. Ribeiro, K. Iha, Determination of the HMX and RDX content in synthesized energetic material by HPLC, FT-MIR, and FT-NIR spectroscopies, Quim. Nova. 27 (2004) 540–544.
[7] M.B. Talawar, R. Sivabalan, T. Mukundan, H. Muthurajan, A.K. Sikder, B.R. Gandhe, A.S. Rao, Environmentally compatible next generation green energetic materials (GEMs), J. Hazard. Mater. 161 (2009) 589–607.
[8] T.M. Klapötke, J. Stierstorfer, Nitration products of 5-Amino-1H-Tetrazole and Methyl-5-Amino-1H-Tetrazoles-structures and properties of promising energetic materials, Helv. Chim. Acta. 90 (2007) 2132–2150.
[9] M. Frankel, L. Grant, J. Flanagan, Historical development of glycidyl azide polymer, J. Propul. Power. 8 (1992) 560–563.
[10] N. Kubota, Combustion of energetic azide polymers, J. Propul. Power. 11 (1995) 677–682.
[11] E.L. Dreizin, M. Schoenitz, Nano-composite energetic powders prepared by arrested reactive milling. US 7,524,335 (2009).
[12] M. Schoenitz, T.S. Ward, E.L. Dreizin, Fully dense nano-composite energetic powders prepared by arrested reactive milling, Proc. Combust. Inst. 30 (2005) 2071–2078.
[13] F.P. Fabbiani, C.R. Pulham, High-pressure studies of pharmaceutical compounds and energetic materials, Chem. Soc. Rev. 35 (2006) 932–942.
[14] Y.L. Shoshin, R.S. Mudryy, E.L. Dreizin, Preparation and characterization of energetic Al-Mg mechanical alloy powders, Combust. Flame 128 (2002) 259–269.
[15] J.J. Granier, M.L. Pantoya, Laser ignition of nanocomposite thermites, Combust. Flame 138 (2004) 373–383.
[16] A. Prakash, A.V. McCormick, M.R. Zachariah, Synthesis and reactivity of a super-reactive metastable intermolecular composite formulation of Al/$KMnO_4$, Adv. Mater. 17 (2005) 900–903.
[17] J.Y. Ahn, J.H. Kim, J.M. Kim, D.W. Lee, J.K. Park, D. Lee, S.H. Kim, Combustion characteristics of high-energy Al/CuO composite powders: the role of oxidizer structure and pellet density, Powder Technol. 241 (2013) 67–73.
[18] J.Y. Ahn, J.H. Kim, J.M. Kim, D.W. Lee, J.K. Park, S.H. Kim, Effect of oxidizer nanostructures on propulsion forces generated by thermal ignition of nano-aluminum-based propellants, J. Nanosci. Nanotechnol. 13 (2013) 7037–7041.
[19] S.B. Kim, K.J. Kim, M.H. Cho, J.H. Kim, K.T. Kim, S.H. Kim, Micro-and nanoscale energetic materials as effective heat energy sources for enhanced gas generators, ACS Appl. Mater. Interfaces 8 (2016) 9405–9412.
[20] J.H. Kim, S.B. Kim, M.G. Choi, D.H. Kim, K.T. Kim, H.M. Lee, H.W. Lee, J.M. Kim, S. H. Kim, Flash-ignitable nanoenergetic materials with tunable underwater explosion reactivity: the role of sea urchin-like carbon nanotubes, Combust. Flame 162 (2015) 1448–1454.
[21] K.J. Kim, H. Jung, J.H. Kim, N.S. Jang, J.M. Kim, S.H. Kim, Nanoenergetic materials-on-multiwalled carbon nanotubes paper chip as compact and flexible igniter, Carbon 114 (2017), 271-223.
[22] T. Tillotson, A. Gash, R. Simpson, L. Hrubesh, J. Satcher, J. Poco, Nanostructured energetic materials using sol–gel methodologies, J. Non Cryst. Solids 285 (2001) 338–345.
[23] T. Tillotson, L. Hrubesh, R. Simpson, R. Lee, R. Swansiger, L. Simpson, Sol–gel processing of energetic materials, J. Non Cryst. Solids 225 (1998) 358–363.
[24] A.E. Gash, T.M. Tillotson, J.H. Satcher Jr., L.W. Hrubesh, R.L. Simpson, New sol–gel synthetic route to transition and main-group metal oxide aerogels using inorganic salt precursors, J. Non Cryst. Solids 285 (2001) 22–28.
[25] S.H. Kim, M.R. Zachariah, Enhancing the rate of energy release from nanoenergetic materials by electrostatically enhanced assembly, Adv. Mater. 16 (2004) 1821–1825.
[26] R. Shende, S. Subramanian, S. Hasan, S. Apperson, R. Thiruvengadathan, K. Gangopadhyay, S. Gangopadhyay, P. Redner, D. Kapoor, S. Nicolich, Nanoenergetic composites of CuO nanorods, nanowires, and Al nanoparticles, Propellants Explos. Pyrotech. 33 (2008) 122–130.
[27] S. Valliappan, J. Swiatkiewicz, J.A. Puszynski, Reactivity of aluminum nanopowders with metal oxides, Powder Technol. 156 (2005) 164–169.
[28] J.Y. Ahn, W.D. Kim, J.H. Kim, J.H. Kim, J.K. Lee, J.M. Kim, S.H. Kim, Gas-phase synthesis of bimetallic oxide nanoparticles with designed elemental compositions for controlling the explosive reactivity of nanoenergetic materials, J. Nanomater. 2011 (2011) 216709.
[29] F.S. Son, B.W. Asay, T.J. Foley, R.A. Yetter, M.H. Wu, G.A. Risha, Combustion of nanoscale Al/$MoO_3$ thermite in microchannels, J. Propul. Power. 23 (2007) 715–721.
[30] B. Mehendale, R. Shende, S. Subramanian, S. Gangopadhyay, P. Redner, D. Kapoor, S. Nicolich, Nanoenergetic composite of mesoporous iron oxide and aluminum nanoparticles, J. Energy Mater. 24 (2006) 341–360.
[31] J. Wang, Z. Qiao, Y. Yang, J. Shen, Z. Long, Z. Li, X. Cui, G. Yang, Core-shell Al-polytetraflouroethylene (PTFE) configurations to enhance reaction kinetics and energy performance for nanoenergetic materials, Chem. Eur. J. 22 (2016) 279–284.
[32] G. Zheng, W. Zhang, R. Shen, J. Ye, Z. Qin, Y. Chao, Three-dimensionally ordered microporous structure enabled nanothermite membrane of $Mn_2O_3$/Al, Sci. Rep. 6 (2016) 22588.
[33] K. Zhang, C. Rossi, M. Petrantoni, N.A. Mauran, Nano initiator realized by integrating Al/CuO-based nanoenergetic materials with a Au/Pt/Cr microheater, J. Microelectromech. Syst. 17 (2008) 832–836.
[34] R.A. Guidotti, P. Masset, Thermally activated ('thermal') battery technology: I. An overview, J. Power Sources 161 (2006) 1443–1449.
[35] S.F. Son, Performance and characterization of nanoenergetic materials at Los Alamos, Mater. Res. Soc. Symp. Proc. 800 (2003), AA5.2.
[36] J.L. Cheng, H.H. Hng, Y.W. Lee, S.W. Du, N.N. Thadhani, Kinetic study of thermal- and impact-initiated reactions in Al–$Fe_2O_3$ nanothermite, Combust. Flame 157 (2010) 2241–2249.
[37] L. Takacs, Self-sustaining reactions induced by ball milling, Prog. Mater Sci. 47 (2002) 355–414.
[38] A. Sossi, E. Duranti, C. Paravan, L.T. DeLuca, A.B. Vorozhtsov, A.A. Gromov, Yu.I. Pautova, M.I. Lerner, N.G. Rodkevich, Non-isothermal oxidation of aluminum nanopowder coated by hydrocarbons and fluorohydrocarbons, Appl. Surf. Sci. 271 (2013) 337–343.
[39] Ž.D. Živković, D. Živković, D. Grujičić, Kinetics and mechanism of the thermal decomposition of $M(NO_3)_2 \cdot nH_2O$ (M = Cu Co, Ni), J. Therm. Anal. Calorim. 53 (1998) 617–623.
[40] I. Morozov, K. Znamenkov, Y.M. Korenev, O. Shlyakhtin, Thermal decomposition of $Cu(NO_3)_2 \cdot 3H_2O$ at reduced pressures, Thermochim. Acta 403 (2003) 173–179.
[41] I. Schildermans, J. Mullens, B. Van der Veken, J. Yperman, D. Franco, L. Van Poucke, Preparation and thermal decomposition of $Cu_2(OH)_3NO_3$, Thermochim. Acta 224 (1993) 227–232.
[42] S. Ryu, W. Lee, S. Park, Thermal decomposition of hydrated copper nitrate [$Cu(NO_3)_2 \cdot 3H_2O$] on activated carbon fibers, Carbon Lett. 5 (2004) 180–185.